

Particle production and Spectra in E802 at BNL-AGS

FLEMMING VIDEBAEK  
Brookhaven National Laboratory  
Upton, New York 11973, USA

*Received by OSTI*

SEP 23 1991

and

THE E802 COLLABORATION  
ANL, BNL, UC Berkeley, UCRiverside, Columbia, Hiroshima  
INS, Kyushu, LLNL, MIT, U.Tokyo

ABSTRACT

The production of  $\pi$ , K, and protons measured in the E802 spectrometer are studied for  $p+A$  and  $Si+A$  collisions. Systematic properties of particle spectra and rapidity density distributions are discussed in terms of centrality and reaction system. A detailed comparison of the data to the RQMD model, which employs the experimental acceptance and cuts, are presented.

## 1. Experimental Setup

The E802 detector consists of a 25msr magnetic spectrometer with PID by time of flight as described in detail in Ref. 1. The beams were  $p$ ,  $^{16}O$ ,  $^{28}Si$  at 14.6 GeV/c accelerated in the BNL tandem-AGS complex. Event characterization was done with a charge particle multiplicity detector (TMA), an array of PbG1 detectors, and a zero degree calorimeter (ZCAL) (ref.2). The hardware triggers consisted of an interaction trigger and a central trigger, which was formed by observing a large multiplicity in the TMA. This central cut corresponds to the upper  $\approx 7\%$  of the multiplicity distribution.

Spectrometer data was taken for  $\theta \approx 5^\circ - 58^\circ$  and for momenta greater than 0.5. The PID using time-of-flight introduces an upper momentum limit of about 2.2 GeV/c for the  $K-\pi$  separation. The acceptance region is roughly  $y = 0.5 - 2.0$  and a low  $p_t$  cut of about 0.2 GeV/c. The upper limit of the  $p_t$  range is rapidity dependent and narrows at the higher rapidities.

## 2. Semi-inclusive data

Semi-Inclusive spectra for  $\pi^\pm$ ,  $K^\pm$  and  $p^\pm$  have been measured in the magnetic spectrometer in the rapidity range of  $y = 0.5 - 2.0$ . Data have previously been reported in ref 3 and 5. In Fig. 1 as an example is shown the invariant cross

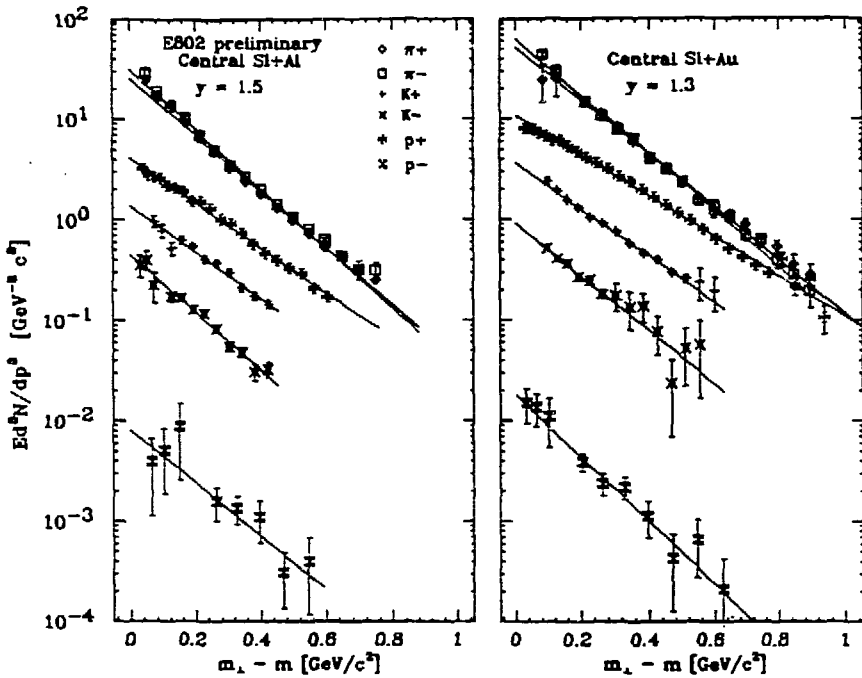


Fig. 1. Invariant cross-sections at  $1.2 \leq y \leq 1.4$  for central Si+Au and central Si+Al. The lines are fits of the form given in Eq. 1.

section  $E \cdot d^3N/dp^3$ , versus  $m_\perp - m$ , where  $m_\perp = \sqrt{p_\perp^2 + m^2}$  and  $m$  is the rest mass. The data are from a rapidity bin of  $\Delta y = 0.2$  centered around  $y=1.5$  and 1.3 for Si+Au and Si+Al respectively. This corresponds to rapidities slightly lower than the central rapidity which for the nucleon-nucleon case is at 1.7. From these data several features can be extracted. Within the acceptance of the experiment the invariant cross sections are quite well described by simple exponentials in the transverse mass  $m_\perp - m$  that is as

$$E \frac{d^3N}{dp^3} \propto e^{-m_\perp/T_0} \quad , \quad (1)$$

where  $T_0$  is the inverse slope parameter. The full drawn curves are the results of exponential fits to the data. It is observed that the  $\pi^+$  and  $\pi^-$  data are nearly identical, and that the  $K^+$  is about 4-5 times the  $K^-$  cross section.

In order to integrate the spectra and extract the rapidity density distributions from the data, it is assumed that the exponential dependence in  $m_\perp$  persists at  $p_\perp$  values  $\leq 0.3\text{GeV}/c$ . This is the procedure used in previous E802 publications.

The data for p+A (ref. 5) are compared with the central Si+Au data in fig 2. Note that the  $\frac{dN}{dy}$  for Si has been divided by 28, i.e. by the mass of the projectile. It is noted that the overall yield of pions increases very little going from p+Be to

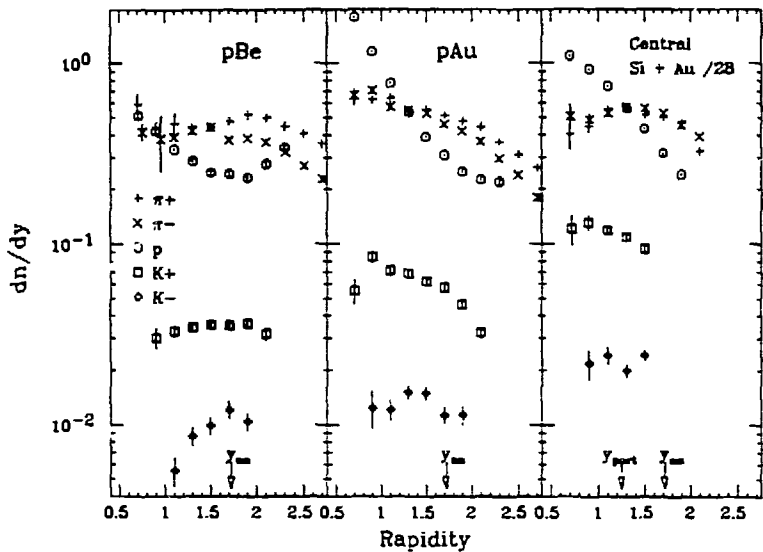


Fig. 2. rapidity densities for  $p+Be$ ,  $p+Au$  and central  $Si+Au$  collisions

central  $Si+Au$  collisions, though the shape does in fact change. In contrast the yield of  $K^+$  increases dramatically, by roughly a factor of 4 for the same reactions. Thus the ratios of  $K^+/\pi^+$  increases from a value in  $p+Be$  ( $\approx 7\%$ ) which is close to the  $p+p$  expectation at this energy to  $\approx 20\%$  for central  $Si+Au$  collisions.

From the previous section it is seen that the  $K^+$  yield was increasing with the mass of the colliding system. A systematic study of the  $K^+/\pi^+$  ratio as function of centrality and target mass have been carried out making use of the ZCAL detector. A detailed analysis of the spectra in ZCAL and their interpretation can be found in ref 4. The energy in the ZCAL reflects the number of projectile participants in the reaction, and thus the centrality of the collision. A simple linear relation exists between energy and the number of projectile participant. Values of  $\frac{dN}{dy}$  were extracted for  $\pi^+$  and  $K^+$  using the method described above and integrated over the rapidity interval  $0.6 < y < 1.4$ . The ratio  $K^+/\pi^+$  in this interval is plotted in fig. 3 for the reaction  $Si+Al$ ,  $Si+Cu$ , and  $Si+Au$  vs number of projectile participants. The general feature is that for a given system the ratio increases with centrality reaching a value of  $\approx 20\%$  for central  $Si+Au$  collisions. The value observed for the peripheral collisions for the lighter targets are close to the value from  $p+p$  reactions, while it is higher for the Au target. The ratio does not depend simply on the participant number but reaches the maximum value for  $Si+Au$  already at a partial overlap of the projectile and target. This is not observed for the lighter targets.

As can be seen from fig 1 the inverse slope parameters depends on the particle kind. That of pions are the lowest and those of protons the highest. The inverse

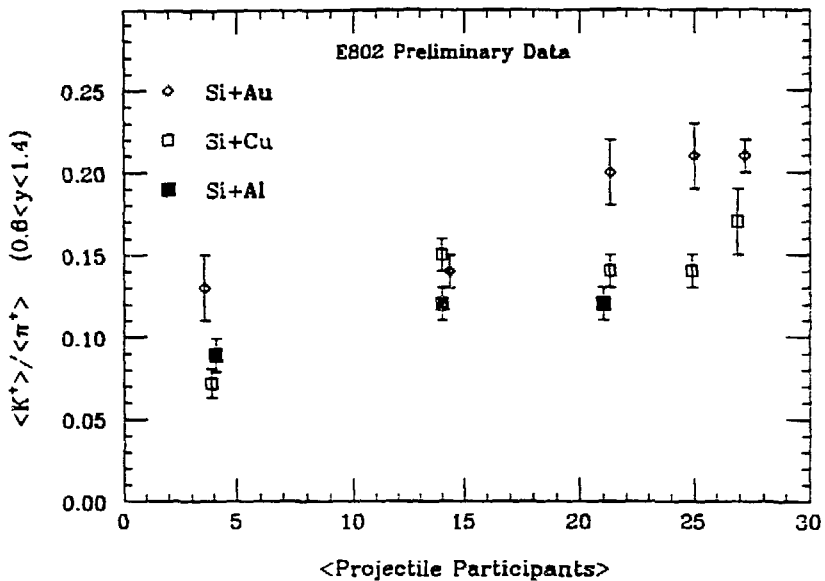


Fig. 3. K/pi ratios versus participant number for Si+Al,Cu and Au reactions.

slope of  $\bar{p}$  are consistent with the of pions. The actual values of  $T_0$  are much more dependent on and sensitive to the assumed shape of the distribution, the acceptance region, and on statistics than the  $\frac{dN}{dy}$ . Since  $T_0$  is further observed to depend on rapidity, much care has to be exercised when comparing values from different reactions and species and bombarding energies. It is though still instructive to look at the reaction dependence. This is shown in fig. 4 for various reactions ranging from  $p+Be$  to central Si+Au for  $\pi^+$ ,  $K^+$ ,  $k^-$ ,  $p$ , and  $\bar{p}$ . A clear trend is observed, namely that the  $T_0$  of pions stays roughly constant around 150 MeV, while that of protons increases rapidly with the mass of the interacting system. That of  $K^+$  also shows an increasing trend and falls between that of pions and protons. The increase of  $T_0$  for protons has been taken as a sign of the importance of rescattering in the reaction process. Independent scattering models like FRITIOF do not include such effects and do not have such dependences.

#### 4. Comparison with RQMD

The Relativistic Quantum Molecular Dynamics (RQMD) model is described in detail in 7. Several prediction of the model at AGS energies has already been published. In brief it uses a covariant description of classical propagation of hadrons and includes quantum effects such as stochastic scattering, particle excitation and decay, and Pauli blocking. The Frankfurt group have calculated 203 events for central collisions, i.e. with an impact parameter of 1 fm,  $^{28}Si + ^{197}Au$  collisions at 14.6 GeV/c. This sample forms the basis for the present analysis (ref. 8).

The emphasis in the present analysis is to treat the model output as data, that is,

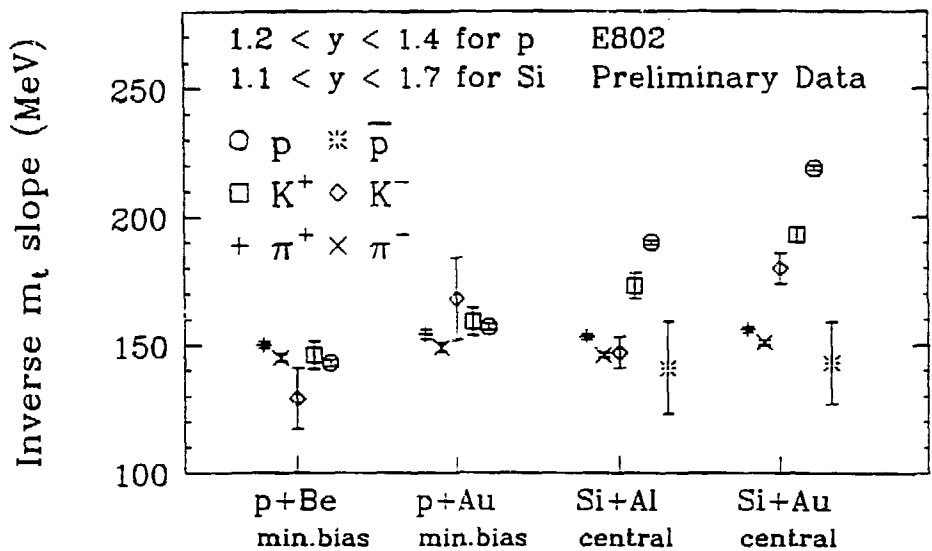


Fig. 4. Comparison of Inverse  $m_t$  slope parameters in  $p+Be$ ,  $p+Au$ , and central  $Si+Al$  and  $Si+Au$  collisions. The errors bars show statistical uncertainties only.

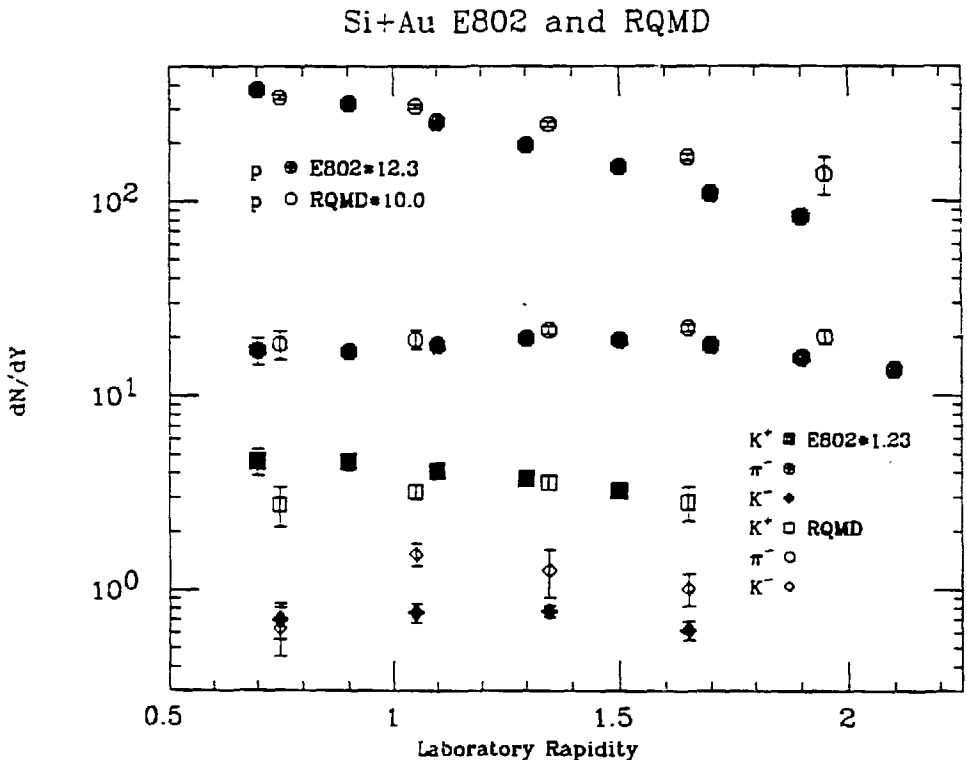


Fig. 5. Rapidity densities for RQMD and E802 data for central  $Si+Au$  collisions.

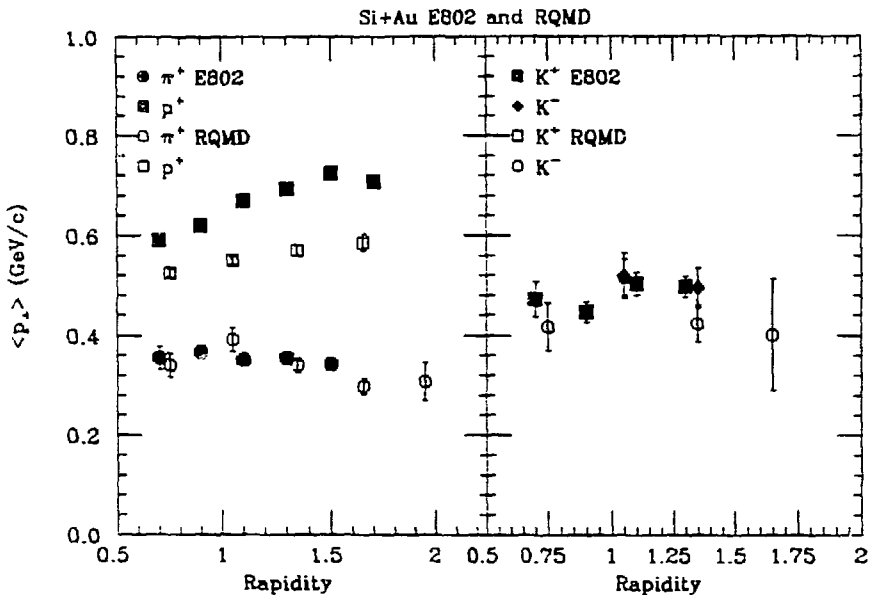


Fig. 6. Average  $p_{\perp}$  extracted from RQMD calculations and E802 data for central Si+Au collisions.

they are subjected to the same acceptance cuts as the E802 spectrometer data and the same data analysis. For each rapidity bin spectra in  $m_{\perp} - m$  were gathered, and fitted to the exponential form of eq. 1 to extract the rapidity densities  $\frac{dN}{dy}$ , the inverse slope parameters  $T_0$  and  $\langle p_{\perp} \rangle$  values. These can then be compared with those extracted from the data.

In the comparison the  $\pi^+$  data have been forced to agree at the low  $m_{\perp}$  values by multiplying the E802 cross sections by 1.23. This partly reflects that the RQMD calculation correspond to more central collision than the E802 TMA triggered cross sections, which samples impact parameters in the range of 0 – 2.5 fm. The comparison of the extrapolated  $\frac{dN}{dy}$  values is shown in fig. 5 for protons,  $\pi^-$ ,  $K^+$  and  $K^-$ . The data are shown as open symbols and the calculations with solid symbols. The  $\pi^+$  results are essentially identical to the  $\pi^-$  data and are not shown.

The overall agreement between the prediction and the data is very good when comparing the  $\frac{dN}{dy}$ . Particular around  $y = 1.3$  both kaons and pions are well described. The model thus reproduces the large  $K^+/\pi^+$  ratios observed using solely a hadronic description of the reaction. Most of the enhancement comes from secondary meson baryon interactions. Some differences are observed. The experimental  $K^+$  data are higher than the model for the smaller rapidities while the  $\frac{dN}{dy}$  for protons of the data falls more rapidly at the larger rapidities. The calculated  $K^-$  yield seems somewhat higher than the data though the statistical uncertainties are quite large.

From the fits in the acceptance region the  $\langle p_{\perp} \rangle$  values were also extracted. They are compared with the data in fig. 6. The striking feature is that the  $\langle p_{\perp} \rangle$  for protons falls well below the data while the values for pions and kaons agree

very well over the whole rapidity range. The RQMD model has many rescatterings involving the baryons, but despite this it does not reproduce the large  $\langle p_\perp \rangle$  observed experimentally for protons.

## 5. Summary

An analysis of the E802 spectrometer data taken for collisions of  $p+A$  and  $^{28}\text{Si}+A$  has been presented. It shows that the properties of pion production change only little with collision system. On the other hand the production of  $K^+$ , as observed by the  $K^+/\pi^+$  ratio, increases smoothly with collision system and centrality. The inverse slope parameters for kaons, but particularly protons increase rapidly with increasing mass of the colliding system. This points to the importance of rescattering in heavy systems, as supported by the comparison with RQMD model. In a solely hadronic scattering description of the collision and decay processes RQMD is able to reproduce quite well the observed rapidity density distributions, and the  $K^+/\pi^+$  ratios for central Si+Au reactions.

## 6. Acknowledgements

This work was supported by the U. S. Department of Energy under contracts with ANL, BNL, Columbia University, LLNL, MIT and UCR, by NASA under contract with the University of California, and by the U.S.-Japan High Energy Physics Collaboration Treaty.

## 8. References

1. T. Abbott, et al., *Nucl. Instrum. and Meth.* **A290** (1990) 41.
2. D. Beavis, et al., *Nucl. Instrum. and Meth.* **A281** (1989) 367.
3. T. Abbott, et al., *Phys. Rev. Lett.* **64** (1991) 847.
4. T. Abbott, et al. "Forward and Transverse Energies in relativistic Heavy Ion collisions at 14.6 GeV/c per Nucleon", *Phys. Rev. C*. In print (1991).
5. T. Abbott, et al., *Phys. Rev. Lett.* **66** (1990) 1567.
6. J. B. Costales, in *Proc. Workshop on Heavy Ion Physics at the AGS*, Brookhaven National Laboratory Report No. BNL-44911 (1990) p. 249.
7. H. Sorge, H. Stocker and W. Greiner, *Ann. Phys. (NY)* **192** (1989) 266 and *Nucl. Phys.* **A498** (1989) p. 657c
8. R. Mattiello, H. Sorge, H. Stocker, W. Greiner, Ole Hansen, B. Moskowitz and F. Videbæk, *in preparation*

## **DISCLAIMER**

This report was prepared as an account of work sponsored by an agency of the United States Government. Neither the United States Government nor any agency thereof, nor any of their employees, makes any warranty, express or implied, or assumes any legal liability or responsibility for the accuracy, completeness, or usefulness of any information, apparatus, product, or process disclosed, or represents that its use would not infringe privately owned rights. Reference herein to any specific commercial product, process, or service by trade name, trademark, manufacturer, or otherwise does not necessarily constitute or imply its endorsement, recommendation, or favoring by the United States Government or any agency thereof. The views and opinions of authors expressed herein do not necessarily state or reflect those of the United States Government or any agency thereof.